NANO-MICRO LETTERS ARTICLE
www.nmletters.org

Fabrication and Evaluation of Low-cost $Cu_2ZnSn(S,Se)_4$ Counter Electrodes for Dye-sensitized Solar Cells

Jie Shen[1], Dingwen Zhang[1], Junjie Li[1], Xiaodong Li[2], Zhuo Sun[1], Sumei Huang[1,*]

(Received 28 August; accepted 28 October; published online 11 November 2013)

Abstract: We explore a simple and eco-friendly approach for preparing CZTS powders and a screen-printing process for $Cu_2ZnSn(S,Se)_4$ (CZTSSe) counter electrodes (CEs) in dye-sensitized solar cells (DSCs). Cu_2ZnSnS_4 (CZTS) nanoparticles have been synthesized via a hydrazine-free solvothermal approach without the assistance of organic ligands. CZTS has been prepared by directly drop-casting the CZTS ink on the cleaned FTO glass, while CZTSSe CEs have been fabricated by screen-printing CZTS pastes, followed by post selenization using Se vapor obtained from elemental Se pellets. The crystal structure, composition and morphology of the as-deposited CZTS nanoparticles and CZTSSe electrodes are characterized by X-ray diffractometer, energy dispersive spectrometer, field emission scanning electron microscopy and transmission electron microscopy. The electrochemical properties of CZTS, CZTSSe and Pt CE based DSCs are examined and analyzed by electrochemical impedance spectroscopy. The prepared CZTS and CZTSSe CEs exhibit a cellular structure with high porosity. DSCs fabricated with CZTSSe CEs achieve a power conversion efficiency of 5.75% under AM 1.5 G illumination with an intensity of 100 mW/cm^2, which is higher than that (3.22%) of the cell using the CZTS CE. The results demonstrate that the CZTSSe CE possesses good electrocatalytic activity for the reduction of charge carriers in electrolyte. The comprehensive CZTSSe CE process is cheap and scalable. It can make large-scale electro-catalytic film fabrication cost competitive for both energy harvesting and storage applications.

Keywords: Copper-zinc-tin-chalcogenide; Selenization; Counter electrode; Dye-sensitized solar cells

Citation: Jie Shen, Dingwen Zhang, Junjie Li, Xiaodong Li, Zhuo Sun and Sumei Huang, "Fabrication and Evaluation of Low-cost Cu_2 $ZnSn(S,Se)_4$ Counter Electrodes for Dye-sensitized Solar Cells", Nano-Micro Lett. 5(4), 281-288 (2013). http://dx.doi.org/10.5101/nml.v5i4.p281-288

Introduction

Great attention has been paid to dye-sensitized solar cells (DSCs) due to its moderate light-to-electricity conversion efficiency, the simple device fabrication process, and low cost [1-4]. Counter-electrode (CE) plays a key role by catalyzing the reduction of the redox species in DSCs. It serves to transfer electrons from external circuit to tri-iodide and iodine in the redox electrolyte. A high-performance DSC requires the CE to be highly catalytic and high conductive. Hence, platinum, which is a good catalyst for the reduction of the redox species, such as tri-iodide/iodide, is usually used as the counter electrode of the DSC. The best platinum counter electrode of a DSC is produced by a high-temperature hydrolysis process. However, the noble platinum remarkably increases the cost of the DSC [5-7]. Thus, many alternative cheap materials have been investigated as the counter electrodes for DSCs.

In previous works, carbon materials and organic polymers were proposed to replace Pt as CE catalysts [8-12]. Then, several inorganic compounds were intro-

[1]Engineering Research Center for Nanophotonics & Advanced Instrument, Ministry of Education, Department of Physics, East China Normal University, North Zhongshan Rd. 3663, Shanghai 200062, P. R. China
[2]Advanced Materials Technology Centre, Singapore Polytechnic, 500 Dover Road 139651 Singapor
*Corresponding author. E-mail: smhuang@phy.ecnu.edu.cn

duced into DSCs as CE catalysts, such as NiN, CoS and NiS [13-15]. Compared with carbon materials and organic polymers, inorganic materials carry many advantages such as broad variety of materials, good plasticity and simple preparation [16]. Thus, many efforts have been made to develop inorganic compounds as an alternative catalysts in DSCs. Copper-zinc-tin-chalcogenides, Cu_2ZnSnS_4 (CZTS), $Cu_2ZnSnSe_4$ (CZTSe) and $Cu_2ZnSn(S,Se)_4$ (CZTSSe) are widely known as promising photovoltaic (PV) p-type absorber materials in thin film solar cells [17-19]. Teodor. K. *et al.* prepared high-quality CZTSSe layers and achieved a high efficiency of 9.66% for CZTSSe-CdS p-n heterojunction solar cells, through addition of significant amount of Se and use of a hydrazine based solution deposition technique [19]. Although this is a very exciting approach, it involves hydrazine, which is toxic and explosive. Recently CZTS(Se) has been suggested as a high efficiency catalysts for tri-iodide reduction and consequently is expected to replace expensive Pt electrode in DSCs [20,21]. For example, Xin *et al.* reported the application of a CZTSSe film as an effective CE in DSCs [20]. Their device indicates good electrocatalytic performance for regeneration of iodide from triiodide in a redox electrolyte and delivers a power conversion efficiency of 7.37%, which is even higher than that (7.04%) of the cell with a Pt CE. They employed a solution-base synthesis approach with the assistance of oleylamine to prepare CZTS nanocrystals at 225℃ in argon. CZTSSe CEs were prepared by sintering of spin-coated CZTS films at 540℃ for 1 h in selenium vapor. For practical photovoltaic (PV) applications, cheap and simple CZTS synthesis methods and roll-to-roll printing processes for CZTS CEs, such as screen-printing and gravure printing, are required to be developed.

In this paper, we report a simple and eco-friendly approach for preparing CZTS powders and a screen-printing process for CZTSSe CEs in DSCs. CZTS nanoparticles were prepared via a hydrazine-free solvothermal approach without the assistance of organic ligands. CZTS CEs were prepared by drop-casting the CZTS ink on the cleaned FTO glass. CZTSSe CEs were grown by screen-printing the CZTS paste containing 5 wt.% of ethyl cellulose on the cleaned FTO glass, followed by heating at 400℃ for 15 min in air and annealing at 500℃ in selenium vapor for 10 min. The electrochemical properties of CZTS, CZTSSe and Pt CE based DSCs were investigated and compared through electrochemical impedance spectroscopy (EIS). Efficient DSCs using CZTSSe as CEs were fabricated. Their efficiency was very close to that of Pt CE based devices.

Experimental

In a typical synthesis of CZTS nanoparticles, 0.2 mmol copper (II) chloride dihydrate, 0.1 mmol zinc (II) chloride, 0.1 mmol tin (II) chloride tetrahydrate and 0.5 mmol thiourea were added into a 50 mL Teflon-lined stainless steel autoclave. Triethylene glycol was filled up to 60% of the total volume. The autoclave was sealed and maintained at 190℃ for 24 h and then allowed to cool to room temperature naturally. The precipitates were filtered off, washed with absolute ethanol. Finally, the products were collected. The as-prepared product was ultrasonic dispersed in absolute ethanol directly to form CZTS inks or followed grinding in a terpineol solution containing 5 wt% of ethyl cellulose to prepare printable CZTS pastes. CZTS CEs were fabricated by drop-casting the ink on the cleaned FTO glass without sintering. CZTSSe CEs were grown by screen-printing the CZTS paste on the cleaned FTO glass, followed by heating at 400℃ for 15 min in air to remove the organic binders. Then, the samples were placed in a homemade selenization system consisted of a graphite box with a sample holder and several pots to hold solid Se pellets [22]. Selenization was carried out at 500℃ for 10 min.

DSCs with CZTS and CZTSSe CEs and thermally prepared Pt were fabricated using screen-printing double-layer TiO_2 served as photoanodes with a total thickness of about 16 μm on the FTO glass plates. The TiO_2 working electrodes were prepared according to the procedures described in our previous work [12,23]. The as-prepared photoanode was dipped in a dye solution (0.5 mM N719 (Solaronix) in acetonitrile and tert-butyl alcohol (volume ratio of 1:1)) at room temperature for 20 h. The cells were sealed with Surlyn 1702 (Dupont) gasket with a thickness of 60 μm. A drop of electrolyte solution (0.05 M I_2, 1 M MPII, 0.5 M Guanidine Thiocyanate and 0.5 M tert-buthylpyridine in acetonitrile) was introduced into the cell by capillarity. Finally, the holes were sealed using the same Surlyn film and a cover glass with a thickness of 0.7 mm.

The structure of the as-prepared CZTS particles and CZTS (Se) electrodes were identified by X-ray diffractometer (XRD, Bruker D8 Davinci instrument, Cu-Kα: $\lambda = 0.15406$ nm). The morphologies of the fabricated particles and CE layers were characterized by field emission scanning electron microscope (FESEM, JSM-7001F, JEOL) and transmission electron microscope (TEM, JSM-2010), respectively. Element analysis of the product was measured by energy dispersive spectrometer (EDS) equipped with the above FESEM. Raman spectrum was recorded by argon ion laser (Spectra-Physics: Stabilite 2017, 514.5 nm, 2 mW) and a triple monochromator (Jobin Yvon: T64000). The thickness of the layers were measured by a profilometer (Dektak 6M). Electrochemical impedance spectroscopy (EIS) measurements of DSCs were recorded with a galvanostat (PG30.FRA2, Autolab, Eco Chemie B. V Utrecht, Netherlands) under illumination 100 mW/cm^2. The frequency range was from 0.1 to 100 KHz. The applied bias and ac amplitude were set at open-circuit

voltage (*Voc*) of the DSCs and 10 mV between the Pt CE and the TiO_2 working electrode, respectively. The obtained spectra were fitted with Z-View software (V3.2) in terms of appropriate equivalent circuits. Photocurrent–voltage ($I-V$) measurements were performed using an AM 1.5 solar simulator equipped with a 1000 W Xenon lamp (Model No. 91192, Oriel, USA). The solar simulator was calibrated by using a standard Silicon cell (Newport, USA). The light intensity was 100 mW/cm^2 on the surface of the test cell. $I-V$ curves were measured using a computer-controlled digital source meter (Keithley 2440). The area of the solar cells is 0.196 cm^2.

Result and discussion

The structure and chemical composition of the as-prepared CZTS were characterized. Figure 1(a) shows the corresponding XRD pattern of the as-prepared CZTS nanoparticles. The major XRD diffraction peaks appealed at 2θ = 28.35°, 32.89°, 47.28°, 50.31° and 56.02° can be attributed to (112), (200), (220), (222) and (312) planes, respectively. All the diffraction peaks were compatible with those of tetragonal CZTS (JCPDS Card, No. 01-075-4122). The EDS spectrum confirmed the sample was exactly composed of Cu, Zn, Sn and S elements, as shown in the Fig. 1(b). The atom ratio of Cu, Zn, Sn, S was determined to be 24.37:10.04:12.39:48.20, which was close to 2:1:1:4. The Raman spectrum of the as-prepared CZTS particles was shown in Fig. 1(c). An intense peak at 338 cm^{-1} was detected, in excellent agreement with published Raman data for CZTS [24]. On the basis of the EDS analysis, we can conclude that the sample is stoichiometric CZTS.

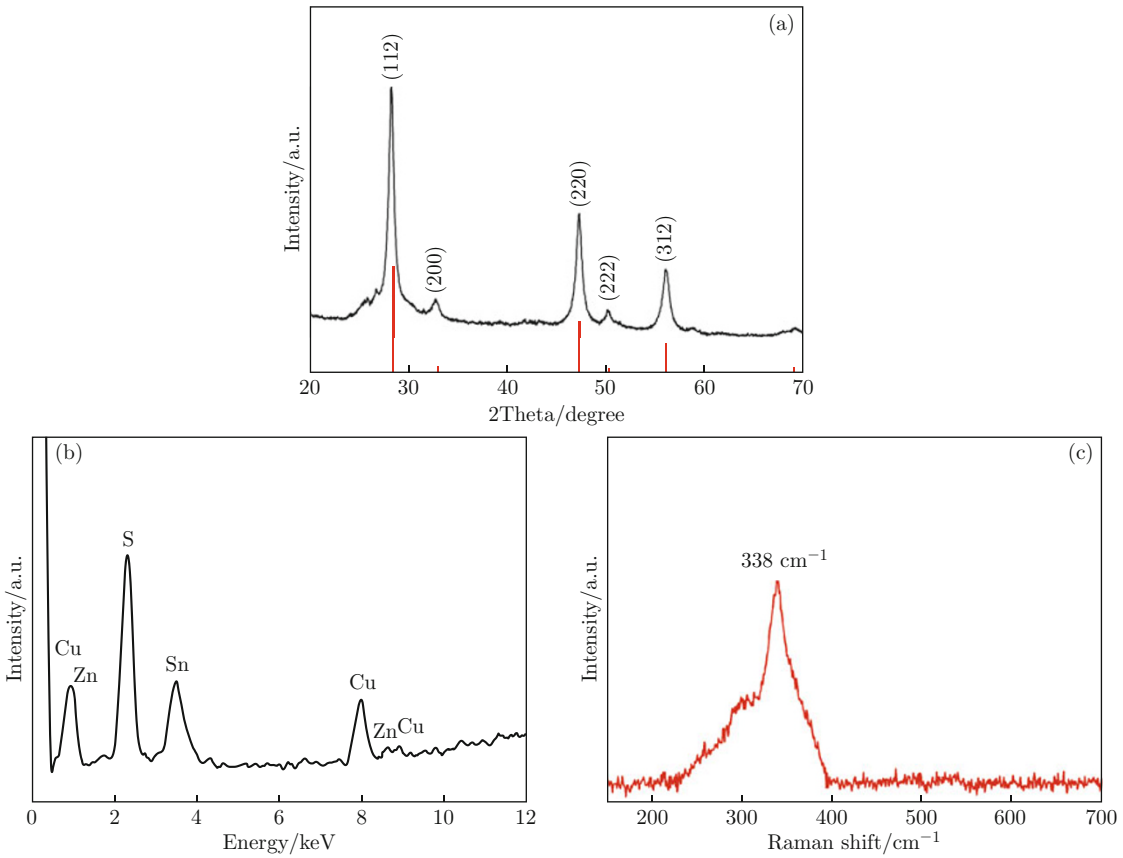

Fig. 1 (a) XRD pattern of as-prepared CZTS nanoparticles. The reference pattern is standard kesterite Cu2ZnSnS4 (JCPDS Card, No. 01-075-4122); (b) EDS and (c) Raman spectra of the as-prepared CZTS nanoparticles.

The morphology of as-prepared CZTS nanoparticles was examined by FESEM and TEM. As shown in Fig. 2(a), the nanoparticles are relatively irregular and the nanoparticles sizes are in the range from approximately 300 nm to 800 nm. The inset of Fig. 2(a) shows the high magnification FESEM image of CZTS nanoparticles, it can be seen that the nanoparticle surfaces are considerably rough. They are composed of numerous tiny nanocrystals with an average crystallite size of 10-20 nm. A high-resolution TEM image (Fig. 2(b)) shows that the nanocrystals have clear lattice fringe with interplanar spacing distance of 3.1 Å, which can be resolved as (112) lattice fringes and agrees well with that determined from the diffraction peak at

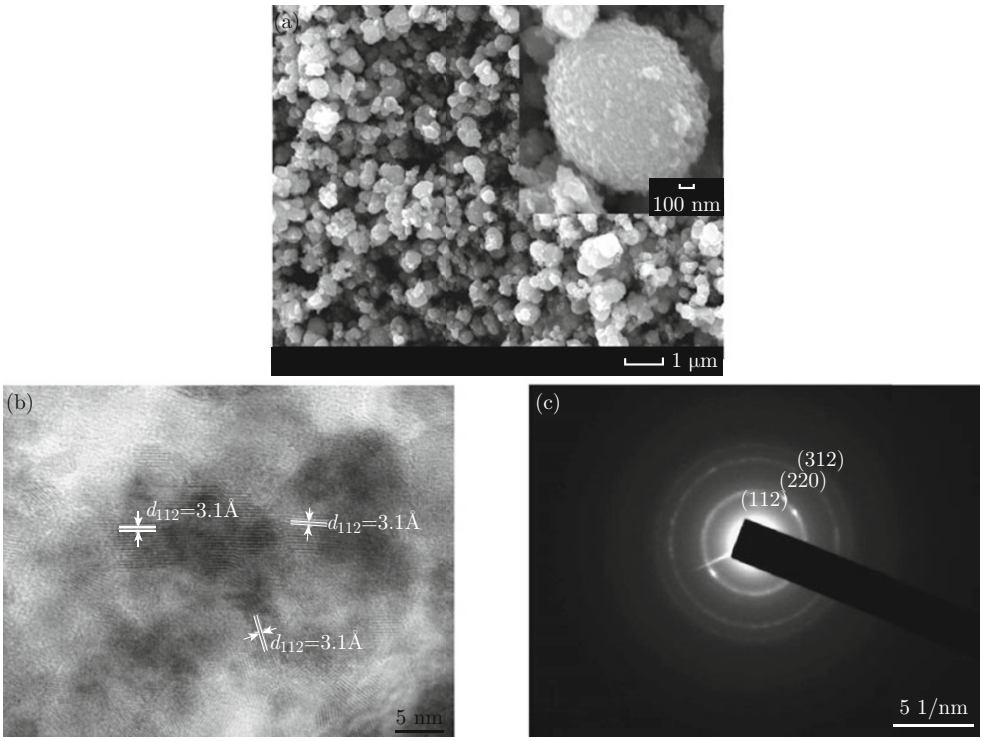

Fig. 2 (a) FESEM image of CZTS nanoparticles; (b) HRTEM image of CZTS nanoparticles; (c) SAED pattern of CZTS nanoparticles.

28.35° in the XRD pattern (Fig. 1(a)) [25,26]. Moreover, the nanocrystals with different growth directions in Fig. 2(b) indicate many nanocrystals in individual nanoparticle. Selected area electron diffraction (SAED) pattern shown in Fig. 2(c) matches the structure of CZTS (JCPDS 01-075-4122) and further reveals that the as-prepared CZTS nanoparticles consist of many nanocrystals, as indicated by the diffraction rings corresponding to the (112), (220) and (312) planes.

Figure 3(a) shows the corresponding XRD pattern of the prepared CZTSSe CE. The XRD diffraction peaks appealed at 2θ = 27.30°, 45.28° and 53.62° can be attributed to (112), (220) and (312) planes of CZTSSe. Diffraction angles of these peaks moved to higher angles compared with those (27.16°, 45.12° and 53.39°) of standard XRD pattern of CZTSe (JCPDS Card, No. 01-070-8930) while remained lower than those of the as-deposited CZTS shown in Fig. 1(a). The shifts were mainly due to the expansion of the unit cell upon replacement of small S with large Se atoms [27,28]. The other XRD diffraction peaks at 2θ = 26.59°, 33.81°, 37.81°, 51.62°, 61.67° and 65.66° are attributed to (110), (101), (200), (211), (310) and (301) planes of SnO_2 substrates. All the diffraction peaks are compatible with those of tetragonal SnO_2 (JCPDS Card, No. 00-046-1088). Figure 3(b) shows an EDS spectrum of CZTSSe CE. The sample was composed of Cu, Zn, Sn, S and Se, and the atom ratio of Cu, Zn, Sn, S, Se was determined to be 24.89:9.27:12.30:2.80:40.33, which is close to that of $Cu_2ZnSn(S,Se)_4$.

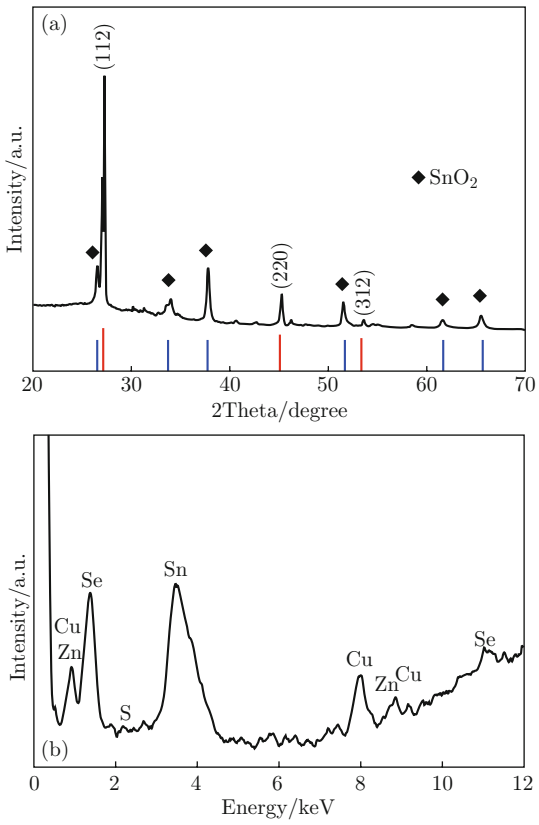

Fig. 3 (a) XRD pattern of as-prepared CZTSSe counter electrode. The reference pattern is standard $Cu_2ZnSnSe_4$ (red, JCPDS Card, No. 01-070-8930) and SnO_2 (blue, JCPDS Card, No. 00-046-1088); (b) EDS spectrum of CZTSSe counter electrode.

Figure 4(a) and 4(b) show the SEM images of CZTS and CZTSSe CE layers prepared on FTO glass substrate, respectively. The thickness of the layers is about 5-6 μm. As can be seen from Fig. 4(a), CZTS presented a cellular structure, albeit with particles of a large size from 500 nm to 1 μm. The particle size was quite similar to that of the as-prepared CZTS powders shown in Fig. 4(a) and 4(b). In the case of CZTSSe CE layer, as shown in Fig. 4(b), CZTSSe also showed a typical cellular structure piled with aggregated particles. Meanwhile, it was evident that some CZTSSe also appeared as a pile of crystals with clear crystalline faces or edges that adhered to one another as a result of sintering and selenization at high temperatures. The CZTSSe exhibited crystals with a size of 2-3 μm. The mesoporous structures shown in CZTS and CZTSSe CEs can be considered as an effective electron transfer network that facilitates the collection and transfer of electrons from the external circuit. And what is more, a few angstrom wide triiodide ions can easily be regenerated at the surface and the pores of the of the CZTS(Se) networks [12,26].

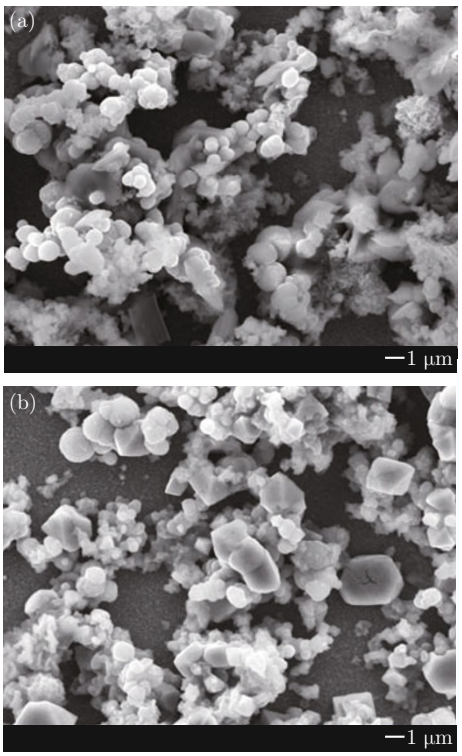

Fig. 4 SEM images of CZTS (a) and CZTSSe (b) layers prepared on FTO glass.

Figure 5 shows the photocurrent density-voltage (J-V) characteristics of DSCs with CZTS and CZTSSe CEs under air mass AM 1.5 simulated solar illumination at 100 mW/cm^2. The performance of DSCs based on chemically deposited Pt/FTO CE was provided for comparison. The detailed information of preparing platinum CE by thermal decomposition is provided in our previous work [29]. The detailed photovoltaic performance parameters are listed in Table 1. It can be seen that DSCs with the conventional Pt CE exhibited a short-circuit current density (J_{sc}) of 15.64 mA/cm^2, open-circuit voltage (V_{oc}) of 0.75 V, fill factor (FF) of 63.58% and conversion efficiency (η) of 7.45%. DSCs with the CZTS and CZTSSe electrodes displayed a comparable V_{oc} of 0.67 V and 0.72 V, but lower FF of 39.72% and 54.44%, lower J_{sc} of 12.11 mA/cm^2 and 14.67 mA/cm^2, and as a consequence, lower η values of 3.22% and 5.75%, respectively. CZTSSe displayed higher conversion efficiency than CZTS, and was more suitable to be used as a catalyst material in DSCs.

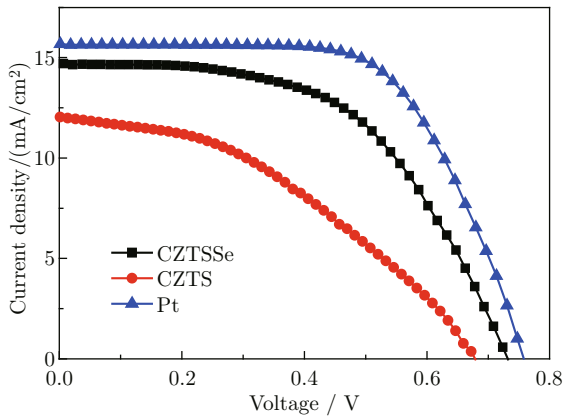

Fig. 5 $I-V$ curves of DSCs fabricated with CZTSSe (solid line) and Pt (dash line) counter electrodes.

Table 1 Photovoltaic parameters of DSCs fabricated with CZTSSe and Pt counter electrodes. The values of R_{ct} are estimated from Fig. 6

CE	R_s	R_{ct1}	Z_w	J_{sc} (mA/cm^2)	V_{oc} (V)	FF (%)	η (%)
Pt	7.4	5.77	4.72	15.64	0.75	63.58	7.45
CZTS	12.7	6.1	33.15	12.11	0.67	39.72	3.22
CZTSSe	11.93	26.32	5.17	14.67	0.72	54.44	5.75

To further investigate the catalytic activities of CZTS and CZTSSe counter electrodes, EIS measurements were carried out. There are many charge-transfer processes in energy conversion in a cell and these processes interact with each other in a complicated manner. The EIS investigation of the DSCs provides valuable information for the understanding of photovoltaic parameters [30-33]. Generally, all the EIS spectrum of DSCs containing liquid electrolyte exhibit three semicircles in the Nyquist plot or three characteristic frequency peaks in the Bode phase plot. The resistance R_{ct1}, R_{ct2} and Z_w are assigned to redox charge transfer at the counter electrode, electron transfer at the TiO_2/dye/electrolyte interface and Warburg diffusion in the electrolyte in the order of decreasing frequency. The ohmic resistance (R_s) is mainly due to the sheet resistance of FTO and connection between FTO and electrodes [34,35].

Figure 6 shows the impedance spectra of DSCs associated with Pt, CZTS and CZTSSe counter electrodes, respectively. The equivalent circuit is shown in the inset of Fig. 6(a). The values of R_{ct2} for the DSCs with various CEs are not quite different from each other because all three kinds of cells were prepared with the same photoanodes. The values of R_{ct1} for the DSCs with Pt and CZTS CEs are very close. However, the use of CZTSSe CE enlarged the R_{ct1} from 5.77 Ω to 26.32 Ω, as shown in Fig. 6(a) and Table 1, indicating poorer catalytic activity of CZTSSe than that of Pt. This enlargement can be attributed to the larger size of CZTSSe crystals than Pt particles and the excessive Se deposited through the selenization process [27]. The size of Pt prepared by thermal decomposition was 5-15 nm [29], which is much smaller than the size of CZTSSe crystals shown in Fig. 4(b). Moreover, the negative phase angle of the high frequency peak is increased from 13.0° for the cell with Pt electrode to 37.9° for the cell with CZTSSe electrode. Correspondingly, the characteristic peak position is shifted from about 5811 Hz to 1212 Hz, which indicates a low electrocatalytic performance for CZTSSe electrode [36]. In contrast, the value of Z_w for the DSC with CZTSSe is very close to that for the Pt based cell, the use of CZTS CE considerably increased the Z_w from 4.72 Ω (with the Pt electrode) to 33.15 Ω. Since CZTS CEs were fabricated by drop-casting the ink on the cleaned FTO glass without sintering, the resulted loose and cellular structure of the CZTS was with high porosity, however, the weak adhesion between CZTS particles and FTO glass led to the highest Z_w and R_s values, resulting in the largest internal series resistance and the lowest FF and thus the poorest η shown in Table 1 [37].

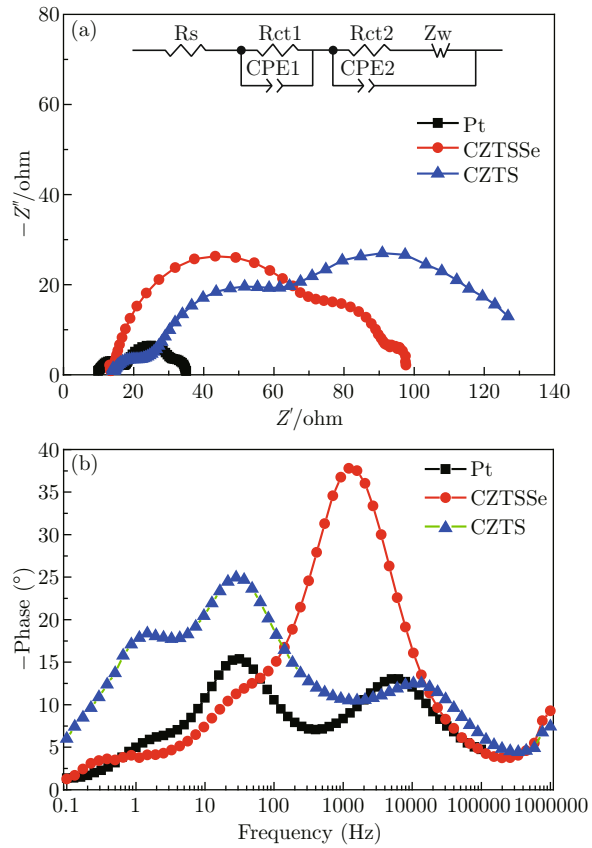

Fig. 6 Impedance spectra of DSCs with Pt, CZTS and CZTSSe counter electrodes. (a) Nyquist plots, (b) Bode phase plots.

In our work, it is found that CZTSSe CE has poorer performance than Pt electrode. This result is different from that reported by Xu *et al.* [20]. They reported that their deposited CZTSSe CE performed better than Pt CE. We think the poorer catalytic property in our grown CZTSSe CE can be attributed to its much larger particle size than Pt particles shown in Fig. 4(b) [27]. In DSCs, the size of Pt prepared by thermal decomposition was about 5-15 nm [29]. The CZTS nanoparticle diameter was approximately (15 ± 6) nm in Lin *et al.*'s work [20]. As shown in Fig. 4(b), the larger CZTSSe particles resulted in greatly loose networks, which caused the higher R_{ct1} listed in Table 1. The higher value of R_{ct1} induced the higher internal series resistance, and resulted in the lower fill factor and the smaller energy conversion efficiency of the CZTSSe-based cells. As we well know, catalytic activity is one of the intrinsic characteristics of a catalyst. It is determined by the electronic structure of the catalyst. To date, however, researchers have not been able to make definitive statements about the electronic structure of the Pt like catalysts or to give a definitive relationship between the electronic structure and the catalytic activity. In addition, for the same kind of catalyst, the catalytic activity can be also affected significantly by the particle size, crystal structure, and so forth [38,39]. Therefore, the catalytic activity of CZTSSe CE can be enhanced by decreasing the size and improving the shape of CZTS powders. The fundamental reasons for the variety of catalytic activities of CZTSSe require further studies.

Conclusions

We have reported on a simple and eco-friendly approach for preparing CZTS powders and a screen-printing process for CZTSSe CEs in DSCs. CZTS nanoparticles were prepared via a hydrazine-free solvothermal approach without the assistance of organic ligands. CZTSSe CEs were prepared by screen-printing CZTS pastes containing 5 wt.% of ethyl cellulose on the cleaned FTO glass, followed by heating in air and selenization in Se vapor. The structure, composition and morphology of the obtained CZTS nanoparticles, CZTS and CZTSSe electrodes were characterized. The electrocatalytic activity of prepared CZTS and CZTSSe electrode was investigated by EIS. DSCs fabricated with prepared CZTSSe counter-electrode achieved an overall conversion efficiency of 5.75% in full sunlight. The device performance could be further

improved by adjusting S/Se ratios and optimizing morphological properties such as particle size and porosity of CZTSSe films.

Acknowledgements

This work was supported by National Natural Science Foundation of China (No. 11274119 and 61275038) and Pujiang Talent Program of Shanghai Science and Technology Commission (No. 11PJ1402700)

References

[1] B. O'Regan and M. Grfitzeli, "A low-cost, high-efficiency solar cell based on dye-sensitized colloidal TiO_2 films", nature 353(6346), 737-740 (1991). http://dx.doi.org/10.1038/353737a0

[2] M. Nazeeruddin, A. Kay, I. Rodicio, R. Humphry-Baker, E. Mueller, P. Liska, N. Vlachopoulos and M. Graetzel, "Conversion of light to electricity by cis-X2bis (2, 2'-bipyridyl-4, 4'-dicarboxylate) ruthenium (II) charge-transfer sensitizers (X= Cl-, Br-, I-, CN-, and SCN-) on nanocrystalline titanium dioxide electrodes", J. Am. Chem. Soc. 115(14), 6382-6390 (1993). http://dx.doi.org/10.1021/ja00067a063

[3] M. Malekshahi Byranvand, Ali Nemati Kharat and Mohammad Hossein Bazargan, "Titania nanostructures for Dye-sensitized solar cells", Nano-Micro Lett. 4(4), 253-266 (2012). http://dx.doi.org/10.3786/nml.v4n4.p253-266

[4] Yafei Zhang, Huijuan Geng, Zhihua Zhou, Jiang Wu, Zhiming Wang, Yaozhong Zhang, Zhongli Li, Liying Zhang, Zhi Yang and Hueyliang Hwang, "Development of inorganic solar cells by nanotechnology", Nano-Micro Lett. 4(2), 124-134 (2012). http://dx.doi.org/10.3786/nml.v4i2.p124-134

[5] T. Ma, X. Fang, M. Akiyama, K. Inoue, H. Noma and E. Abe, "Properties of several types of novel counter electrodes for dye-sensitized solar cells", J. Electroanal. Chem. 574(1), 77-83 (2004). http://dx.doi.org/10.1016/j.jelechem.2004.08.002

[6] P. Li, J. Wu, J. Lin, M. Huang, Z. Lan and Q. Li, "Improvement of performance of dye-sensitized solar cells based on electrodeposited-platinum counter electrode", Electrochim. Acta 53(12), 4161-4166 (2008). http://dx.doi.org/10.1016/j.electacta.2007.12.073

[7] G. Calogero, P. Calandra, A. Irrera, A. Sinopoli, I. Citro and G. Di Marco, "A new type of transparent and low cost counter-electrode based on platinum nanoparticles for dye-sensitized solar cells", Energy Environ. Sci. 4(5), 1838-1844 (2011). http://dx.doi.org/10.1039/c0ee00463d

[8] A. Kay and M. Grätzel, "Low cost photovoltaic modules based on dye sensitized nanocrystalline titanium dioxide and carbon powder", Sol. Energy Mater. Sol. Cells 44(1), 99-117 (1996). http://dx.doi.org/10.1016/0927-0248(96)00063-3

[9] J. Roy-Mayhew, D. Bozym, C. Punckt and I. Aksay, "Functionalized graphene as a catalytic counter electrode in dye-sensitized solar cells", ACS Nano 4(10), 6203-6211 (2010). http://dx.doi.org/10.1021/nn1016428

[10] Q. Tai, B. Chen, F. Guo, S. Xu, H. Hu, B. Sebo and X. Z. Zhao, "In situ prepared transparent polyaniline electrode and its application in bifacial dye-sensitized solar cells", ACS Nano 5(5), 3795-3799 (2011). http://dx.doi.org/10.1021/nn200133g

[11] K. M. Lee, C. Y. Hsu, P. Y. Chen, M. Ikegami, T. Miyasaka and K. C. Ho, "Highly porous PProDOT-Et_2 film as counter electrode for plastic dye-sensitized solar cells", Phys. Chem. Chem. Phys. 11(18), 3375-3379 (2009). http://dx.doi.org/10.1039/b823011k

[12] D. Zhang, X. Li, H. Li, S. Chen, Z. Sun, X. Yin and S. Huang, "Graphene-based counter electrode for dye-sensitized solar cells", Carbon 49(15), 5382-5388 (2011). http://dx.doi.org/10.1016/j.carbon.2011.08.005

[13] Q. Jiang, G. Li, S. Liu and X. Gao, "Surface-nitrided nickel with bifunctional structure as low-cost counter electrode for dye-sensitized solar cells", J. Phys. Chem. C 114(31), 13397-13401 (2010). http://dx.doi.org/10.1021/jp1035184

[14] M. Wang, A. M. Anghel, B. Marsan, N. L. Cevey Ha, N. Pootrakulchote, S. M. Zakeeruddin and M. Grätzel, "CoS supersedes Pt as efficient electrocatalyst for triiodide reduction in dye-sensitized solar cells", J. Am. Chem. Soc. 131(44), 15976-15977 (2009). http://dx.doi.org/10.1021/ja905970y

[15] H. Sun, D. Qin, S. Huang, X. Guo, D. Li, Y. Luo and Q. Meng, "Dye-sensitized solar cells with NiS counter electrodes electrodeposited by a potential reversal technique", Energy Environ. Sci. 4(8), 2630-2637 (2011). http://dx.doi.org/10.1039/c0ee00791a

[16] M. Wu, X. Lin, A. Hagfeldt and T. Ma, "Low-cost molybdenum carbide and tungsten carbide counter electrodes for dye-sensitized solar cells", Angew. Chem. Int. Ed. 50(15), 3520-3524 (2011). http://dx.doi.org/10.1002/anie.201006635

[17] H. Katagiri, K. Jimbo, W. S. Maw, K. Oishi, M. Yamazaki, H. Araki and A. Takeuchi, "Development of CZTS-based thin film solar cells", Thin Solid Films 517(7), 2455-2460 (2009). http://dx.doi.org/10.1016/j.tsf.2008.11.002

[18] G. Zoppi, I. Forbes, R. Miles, P. J. Dale, J. J. Scragg and L. M. Peter, "$Cu_2ZnSnSe_4$ thin film solar cells produced by selenisation of magnetron sputtered precursors", Prog. Photovoltaics 17(5), 315-319 (2009). http://dx.doi.org/10.1002/pip.886

[19] T. K. Todorov, K. B. Reuter and D. B. Mitzi, "High-efficiency solar cell with earth-abundant liquid-processed absorber", Adv. Mater. 22(20), E156-E159 (2010). http://dx.doi.org/10.1002/adma.200904155

[20] X. Xin, M. He, W. Han, J. Jung and Z. Lin, "Low-cost copper zinc tin sulfide counter electrodes for high-efficiency dye-sensitized solar cells", Angew. Chem. Int. Ed. 50(49), 11739-11742 (2011). http://dx.doi.org/10.1002/anie.201104786

[21] Y. F. Du, J. Q. Fan, W. H. Zhou, Z. J. Zhou, J. Jiao and S. X. Wu, "One-step synthesis of stoichiomet-

ric $Cu_2ZnSnSe_4$ as counter electrode for dye-sensitized solar cells", ACS Appl. Mater. Inter. 4(3), 1796-1802 (2012). http://dx.doi.org/10.1021/am3000616

[22] J. Shi, Z. Li, D. Zhang, Q. Liu, Z. Sun and S. Huang, "Fabrication of Cu (In, Ga) Se_2 thin films by sputtering from a single quaternary chalcogenide target", Prog. Photovoltaics. 19(2), 160-164 (2011). http://dx.doi.org/10.1002/pip.1001

[23] X. Li, D. Zhang, S. Chen, H. Zhang, Z. Sun, S. Huang and X. Yin, "Dye-sensitized solar cells with higher Jsc by using polyvinylidene fluoride membrane counter electrodes", Nano-Micro Lett. 3(3), 195-199 (2011). http://dx.doi.org/10.3786/nml.v3i3.p195-199

[24] H. Yoo and J. Kim, "Comparative study of Cu_2ZnSnS_4 film growth", Sol. Energ. Mater. Sol. C 95(1), 239-244 (2011). http://dx.doi.org/10.1016/j.solmat.2010.04.060

[25] S. Han, M. Kong, Y. Guo and M. Wang, "Synthesis of copper indium sulfide nanoparticles by solvothermal method", Mater. Lett. 63(13), 1192-1194 (2009). http://dx.doi.org/10.1016/j.matlet.2009.02.032

[26] C. Zou, L. Zhang, D. Lin, Y. Yang, Q. Li, X. Xu, X. Chen and S. Huang, "Facile synthesis of Cu_2ZnSnS_4 nanocrystals", Cryst. Eng. Comm. 13(10), 3310-3313 (2011). http://dx.doi.org/10.1039/c0ce00631a

[27] J. He, L. Sun, S. Chen, Y. Chen, P. Yang and J. Chu, "Composition dependence of structure and optical properties of Cu_2ZnSn (S, Se)$_4$ solid solutions: An experimental study", J. Alloy Compd. 511(1), 129-132 (2011). http://dx.doi.org/10.1016/j.jallcom.2011.08.099

[28] C. Jiang, J. S. Lee and D. V. Talapin, "Soluble precursors for $CuInSe_2$, $CuIn_{1-x}$ Ga_xSe_2, and Cu_2ZnSn (S, Se)$_4$ based on colloidal nanocrystals and molecular metal chalcogenide surface ligands", J. Am. Chem. Soc. 134(11), 5010-5013 (2012). http://dx.doi.org/10.1021/ja2105812

[29] D. Zhang, X. Li, S. Chen, F. Tao, Z. Sun, X. Yin and S. Huang, "Fabrication of double-walled carbon nanotube counter electrodes for dye-sensitized solar cells", J. Solid State Electrochem. 14(9), 1541-1546 (2010). http://dx.doi.org/10.1007/s10008-009-0982-3

[30] J. Bisquert, "Theory of the impedance of electron diffusion and recombination in a thin layer", J. Phys. Chem. B 106(2), 325-333 (2002). http://dx.doi.org/10.1021/jp011941g

[31] A. Fillinger, D. Soltz and B. Parkinson, "Dye sensitization of natural anatase crystals with a ruthenium-based dye", J. Solid State Electrochem. 149(9), A1146-A1156 (2002). http://dx.doi.org/10.1149/1.1495497

[32] Q. Wang, J. E. Moser and M. Grätzel, "Electrochemical impedance spectroscopic analysis of dye-sensitized solar cells", J. Phys. Chem. B 109(31), 14945-14953 (2005). http://dx.doi.org/10.1021/jp052768h

[33] T. Hoshikawa, M. Yamada, R. Kikuchi and K. Eguchi, "Impedance analysis of internal resistance affecting the photoelectrochemical performance of dye-sensitized solar cells", J. Solid State Electrochem. 152(2), E68-E73 (2005). http://dx.doi.org/10.1149/1.184776

[34] C. Longo, J. Freitas and M. A. De Paoli, "Performance and stability of TiO_2 dye solar cells assembled with flexible electrodes and a polymer electrolyte", J. Photoch. Photobio. A 159(1), 33-39 (2003). http://dx.doi.org/10.1016/S1010-6030(03)00106-0

[35] M. Bernard, H. Cachet, P. Falaras, A. Hugot-Le Goff, M. Kalbac, I. Lukes, N. Oanh, T. Stergiopoulos and I. Arabatzis, "Sensitization of TiO_2 by Polypyridine Dyes Role of the Electron Donor", J. Solid State Electr. 150(3), E155-E164 (2003). http://dx.doi.org/10.1149/1.1543951

[36] G. Zhu, L. Pan, T. Lu, T. Xu and Z. Sun, "Electrophoretic deposition of reduced graphene-carbon nanotubes composite films as counter electrodes of dye-sensitized solar cells", J. Mater. Chem. 21(38), 14869-14875 (2011). http://dx.doi.org/10.1039/c1jm12433a

[37] L. Han, N. Koide, Y. Chiba, A. Islam, R. Komiya, N. Fuke, A. Fukui and R. Yamanaka, "Improvement of efficiency of dye-sensitized solar cells by reduction of internal resistance", Appl. Phys. Lett. 86(21), 213501-213501-3 (2005). http://dx.doi.org/10.1063/1.1925773

[38] E. Ramasamy, W. J. Lee, D. Y. Lee and J. S. Song, "Nanocarbon counterelectrode for dye sensitized solar cells", Appl. Phys. Lett. 90(17), 173103 (2007). http://dx.doi.org/10.1063/1.2731495

[39] A. R. Ko, J. K. Oh, Y. W. Lee, S. B. Han and K. W. Park, "Characterizations of tungsten carbide as a non-Pt counter electrode in dye-sensitized solar cells", Mater. Lett. 65(14), 2220-2223 (2011). http://dx.doi.org/10.1016/j.matlet.2011.04.062